Planet. Space Sci. 1973, Vol. 21, pp. 2027 to 2037. Pergamon Press. Printed in Northern Ireland

# PARTICLE MOTION AND CURRENTS IN THE NEUTRAL SHEET OF THE MAGNETOSPHERIC TAIL

M. I. PUDOVKIN and N. A. TSYGANENKO
Physical Institute, Leningrad State University, Leningrad 199164, U.S.S.R.

(*Received in final form* 26 *February* 1973)

**Abstract**—The trajectories of plasma-sheet protons are computed numerically in magnetic-field models which simulate the neutral-sheet-type configuration observed in experiments. No electric field is included, in contrast with the reconnection theory. Entering the neutral sheet and then exiting from it, the particle performs an ordered displacement across the tail. A continuous interchange between the neutral and plasma sheets will give rise to an electric current which may be responsible for the observed magnetic-field configuration. An estimate of this current is made from the tension balance requirement, showing that a substantial anisotropy of the plasma-sheet pressure is necessary to maintain the steady state. It is shown that the neutral sheet itself can be a source of such an anisotropy, due to the non-adiabatic behaviour of protons. Other anisotropy origins are discussed briefly.

## 1. INTRODUCTION

Being one of the most significant features of the solar-wind interaction with the geomagnetic field, the magnetospheric tail became an object of extensive study eight years ago, when Ness *et al.* (1964) reported the field lines behind the Earth to be stretched away from the Sun. Though a wealth of experimental data on the magnetotail structure and dynamics has been accumulated up to now, a number of fundamental questions are far from being clear.

This paper deals with one such problem, namely, the nature of the tail current system which causes the geomagnetic field configuration observed by satellites.

From the existing magnetotail theories, one should note a well-known reconnection model developed recently by Hill and Dessler (1971). The solar-wind plasma particles leak down the tail exhibiting a drift motion towards the neutral sheet with subsequent loss in the magnetosheath. However, there is experimental evidence (Behannon, 1970; Fairfield and Ness, 1970) of the vertical magnetic field component which is comparatively high in the near tail region up to geocentric distances of 30–40$R_E$. Hence, the mechanism of particle motion across the tail should be more complicated than the simplest one assumed by Hill and Dessler.

Beard *et al.* (1970) proposed a model which explains the current sheet in the tail with a drift of particles, due to the vertical-field-component gradient observed experimentally. However, it is known from a general theory (Longmire, 1963) that the gradient-drift currents in the guiding-centre approximation are cancelled completely by part of the magnetization currents. It should be stressed also that the adiabatic drift motion of the particles is very unlikely to exist in the fluctuating field of the neutral sheet.

We shall consider in this paper a possible mechanism which may be responsible for the observed neutral-sheet currents, and requires an anisotropic pressure in the plasma sheet. It will be shown that the neutral sheet itself can be a source of such an anisotropy, due to the non-adiabatic behaviour of protons.

## 2. PARTICLE TRAJECTORIES IN A MODEL PLASMA SHEET

Experimental data show the typical magnetotail structure to consist of three different zones, specifically, (a) the high-latitude region of intense and stable magnetic field, (b) a

thick (up to 10–12$R_E$) sheet of field depression coincident with the plasma sheet, and (c) enveloped by the latter a thin layer of the field reversal, or the neutral sheet.

For the purpose of better understanding the main features of particle motion in the plasma sheet, we have computed the trajectories of a proton in several idealized two-dimensional magnetic-field models, which are similar in their general outlines to an average picture observed in space. The horizontal magnetic-field component $B_x = B_x(z)$ was chosen as an odd function of $z$ which is relatively small in a close vicinity of the equatorial plane $z = 0$. Increasing steeply with $z$, it reaches a value of 5–10$\gamma$ and then varies more slowly, simulating the comparatively broad magnetic-field depression of the plasma sheet.

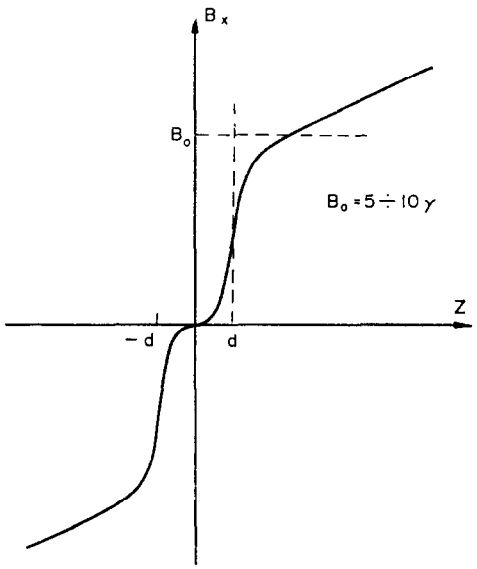


FIG. 1(a). THE HORIZONTAL MAGNETIC FIELD COMPONENT AS A FUNCTION OF DISTANCE FROM THE NEUTRAL-SHEET PLANE IN THE TWO-DIMENSIONAL MODEL.

The vertical component $B_z = B_z(x)$ was taken as a smooth, monotonically-decreasing function in accordance with experimental evaluations by Behannon (1970). As an example, two curves are shown in Figs. 1(a) and (b) which represent the magnetic-field configuration in one of the models considered. The corresponding functions are ($x$ and $z$ in Earth radii):

$$B_x(z) = \begin{cases} B_0 \cdot \dfrac{(z/d)^4}{1 + (z/d)^4} \operatorname{sign}(z) & \text{if } |z| < 2d \\ (a\,|z| + b) \operatorname{sign}(z) & \text{if } |z| > 2d \end{cases} \tag{1}$$

$$B_z(x) = 1{\cdot}67 \,.\, 10^3 (x + 12{\cdot}7)^{-3} \tag{2}$$

where the parameters $B_0$ and $d$ determine the field magnitude just above the neutral sheet, and its thickness, respectively. The parameters $a$ and $b$ were chosen from the requirement of $B_x(z)$ continuity, so that in 2–3$R_E$ (the approximate half-thickness of the plasma sheet) the horizontal component increases linearly from $\sim 10\gamma$ up to $\sim 20\gamma$, the latter value being typical for the high-latitude magnetotail. All the computations were performed using a fourth-order Runge–Kutta method which allowed us to trace the proton trajectory corresponding to $\sim$20 min of its motion, with high accuracy.

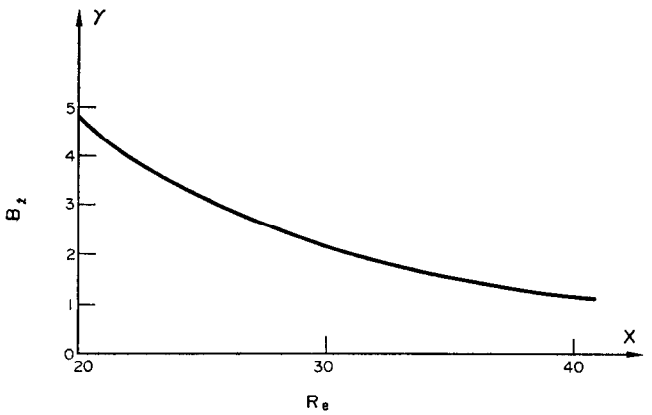


FIG. 1(b). THE VERTICAL FIELD COMPONENT DISTRIBUTION ALONG THE TAIL IN THE SAME MODEL.

Though rather complicated, all the trajectories have several common features which are as follows. Starting from a point in the plane $z = 0$, the particle is oscillating for some time inside the neutral sheet. Due to the transverse field component $B_z$, the oscillations are accompanied by a circular twisting of the trajectory around the $z$-direction. After some oscillations, the particle is ejected from the neutral sheet into the plasma sheet, then reflects at a certain mirror point and returns back, etc. In its essential features this type of motion resembles the one described by Shabansky (1971) and Speiser (1965, 1967) for a case of rather strong crosstail electric field. However, our model does not include any electric field; this leads to an enhancement of the time spent by the particle in the neutral sheet. It is of importance that, in all cases computed, entrance and exit points are spaced by an interval of the order of $\Delta y \sim r_L$ across the tail, where $r_L$ is the gyroradius in the transverse field $B_z$. If the pitch-angle of a particle incident on the neutral sheet is small, the displacement reaches its maximum value of $\sim 2r_L$. The last statement is evident at least qualitatively from Fig. 2, which shows a part of a 10 keV proton trajectory computed in the magnetic field model (1) and (2) with the parameters: $B_0 = 20\gamma$, $d = 1{\cdot}5R_E$ (smaller values of $d$, for example $d = 0{\cdot}1R_E$, yield the same results). This is consistent with the result by Alexeev and Kropotkin (1970): $\Delta y = 2r_L \cos\theta$, where $\theta$ is the pitch-angle. However, they have assumed the neutral sheet to be infinitely thin compared with particle gyroradius, whereas for the thermal proton component it is not the case.

The point here is that each act of entrance–exit of the particle results in its ordered

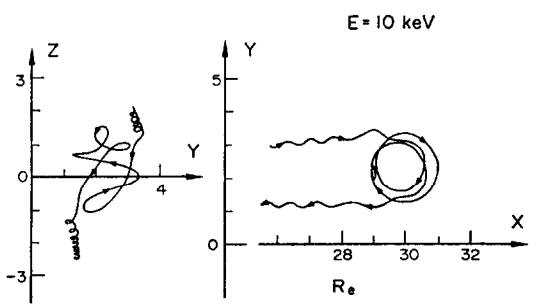


FIG. 2. A PART OF A PROTON TRAJECTORY COMPUTED IN THE PLASMA-SHEET MODEL (1) AND (2).

displacement, so the continuous interchange between the neutral and plasma sheets will give rise to an electric current. Its role in the observed tail current system will be made clear in the next section.

It should be noted that our field model includes the plasma-sheet depression and, hence, a gradient of the magnetic field in the $z$-direction. The gradient drift of the particle in the plasma sheet is directed oppositely to its displacement in the neutral sheet. The relative magnitude of both effects will also be discussed below.

### 3. A TENSION BALANCE IN THE STATIONARY PLASMA SHEET*

We shall now estimate the current density with the aid of a simplified model sketched in Fig. 3. A plasma sheet, with field-aligned and transverse pressure components being

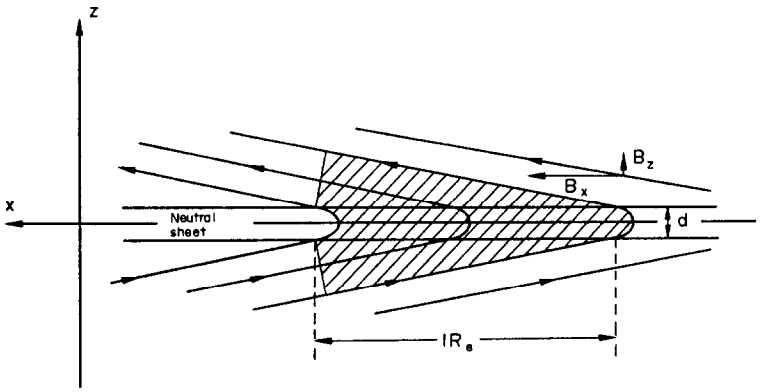


FIG. 3. A SCHEMATIC FIELD-LINE CONFIGURATION IN THE VICINITY OF THE NEUTRAL SHEET.

respectively $p_{\parallel}$ and $p_{\perp}$, envelopes a thin neutral sheet of thickness $d$. We shall neglect the magnetic pressure in the neutral sheet and the gradient of the vertical field component $\partial B_z/\partial x$ with respect to $\partial B_x/\partial z$, as confirmed by experiments (Behannon, 1970). Due to the absence of electric field, assumed in our model, there is also no dynamic flow pressure. Denoting by $B_x$ and $B_z$ the components of the plasma-sheet magnetic field $\vec{B}_{ps}$, we obtain the total force per unit sheet width and length, acting in the $x$-direction on the volume of plasma shown by hatching in Fig. 3:

$$F_x = 2(p_{\perp} - p_{\parallel})(B_x B_z/B_{ps}^2) - d(\partial p_n/\partial x) + iB_z/c. \tag{3}$$

The second term on the right accounts for the gradient of the neutral-sheet plasma pressure $p_n$, and the last term is the electrodynamic tension, where $i$ is the current per unit length of the sheet. Noting that a steady state implies the balance condition $F_x = 0$, we obtain thus:

$$i = 2c(p_{\parallel} - p_{\perp})(B_x/B_{ps}^2) + (cd/B_z)(\partial p_n/\partial x). \tag{4}$$

Inserting (4) into Maxwell's equation:

$$B_{ps} \approx B_x = 2\pi i/c$$

and removing $p_n$ with the aid of the transverse pressure balance condition:

$$p_n = B_t^2/8\pi = B_{ps}^2/8\pi + p_{\perp} \tag{5}$$

* After the present work was completed, a recent paper by Rich *et al.* (1972) became available, which contains a more general treatment of the stress balance problem. The question is also developed by Schindler (1972).

where $B_t$ is the high-latitude tail-field intensity, we find:

$$p_{\parallel} - p_{\perp} = B_{ps}^2/4\pi - (dB_{ps}B_t/8\pi B_z)(\partial B_t/\partial x). \tag{6}$$

If the second term on the right tends to zero, in the case of uniformity in the $x$-direction ($\partial B_t/\partial x \to 0$) and/or a very thin neutral sheet ($d \to 0$), we come to the well-known condition of the firehose instability discussed recently by Siscoe (1972). Denoting: $p_{\parallel}/p_{\perp} = \alpha$; $B_t/B_{ps} = \delta$; $(d/B_z)(\partial B_t/\partial x) = k$, we have, combining (6) with the second equation from (5):

$$\alpha = (\delta^2 - k\delta + 1)/(\delta^2 - 1). \tag{7}$$

Now we can estimate the plasma-sheet pressure anisotropy, substituting in (7) typical values of the magnetotail parameters. Fairfield and Ness (1970) observed a 40–50 per cent decrease of the field magnitude during IMP-3 entrance into the plasma sheet from the high-latitude region (see their Fig. 7). According to these data we take $\delta \sim 2$. The high-latitude tail-field gradient and the vertical field component in the neutral sheet can be evaluated using the results by Behannon (1970): $\partial B_t/\partial x \sim 0{\cdot}5\gamma/R_E$, $B_z \sim 2\gamma$ in the near-tail region. Assuming then $d \sim 0{\cdot}1R_E$, we have from (7) $\alpha \approx 1{\cdot}6$. We see thus a remarkable anisotropy is necessary in the plasma sheet, to maintain a stationary configuration. Physically this means that the neutral-sheet pressure gradient alone is not large enough to balance the Ampère force; to get an additional tension one should introduce the anisotropy, with small pitch-angles prevailing. This conclusion is consistent with the experimental data from Vela satellites (Hones *et al.*, 1971) which give evidence of the plasma-sheet particles forming sharp field-aligned beams. A possible cause of the plasma-sheet anisotropy will be considered in the next section.

Now it is of interest to calculate from (4) a mean particle displacement per one entrance–exit act, and compare the result with that of Section 2. We shall suppose the coupling between the protons and electrons to be insufficient, so all the speculations are valid for the particles of both species separately.

Note, first of all, that the net current which produced the plasma-sheet field $\vec{B}_{ps}$ is the sum of the neutral-sheet drift current and the magnetization one distributed just outside the region of the magnetic field reversal. The magnetization current can be derived in our case directly from its definition. Let us consider a closed contour *abcda* shown in Fig. 3, which surrounds the element $S$ of unit length of the neutral sheet. Integration over the area inside the contour yields the magnetization current:

$$i_m = c\int_S \operatorname{rot} \vec{M}\, \mathrm{d}s = c\oint_{abcda} M_1\, \mathrm{d}l. \tag{8}$$

As we do not consider in (8) the currents inside the neutral sheet, let us suppose here, formally: $\vec{M} = 0$ (strictly speaking, vector $\vec{M}$ is not defined in this region). If we neglect gradients in the $x$-direction, then integrals along paths *bc* and *da* will cancel each other; in the regions outside the neutral sheet the magnetization vector is simply $\vec{M} = -(p_{\perp}/B_{ps}^2)\vec{B}_{ps}$. We obtain thus from (8):

$$i_m = -2cp_{\perp}B_x/B_{ps}^2. \tag{9}$$

We can separate now the drift part of the net current given by (4) as:

$$i_{dr\ ns} = 2cp_{\parallel}B_x/B_{ps}^2 \approx 2cp_{\parallel}/B_{ps} \tag{10}$$

(the gradient term in (4) is neglected as being small).

Notice that the number of particles entering, per second, the shaded element of the neutral sheet in Fig. 3, per unit $x$–$y$ area, is:

$$\nu \approx n\bar{v}_{\parallel}(B_z/B_{ps})$$

where $n$ is the particle concentration and $\bar{v}_{\parallel}$ is the r.m.s. parallel velocity. Denoting the unknown displacement $\Delta y$, we have the drift current in the neutral sheet as:

$$i_{dr\ ns} = e\nu\,\Delta y = en\bar{v}_{\parallel}\,\Delta y(B_z/B_{ps}).$$

Excluding $i_{dr\ ns}$ with the help of (10), we obtain:

$$\Delta y = 2cB_x p_{\parallel}/(en\bar{v}_{\parallel}B_z B_{ps}) \approx 2mc\bar{v}_{\parallel}/eB_z = 2r_L \cos\theta \tag{11}$$

in agreement with the result of Section 2.

We turn now to the effect of the plasma-sheet-magnetic-field gradient which leads to negative displacement of a particle outside the neutral sheet. It is easy to obtain the drift current density in the plasma sheet as:

$$j_{dr\ ps} = cp_{\perp}(\partial/\partial z)(1/B_{ps}).$$

Integration over the cross-section of the plasma sheet (except the neutral sheet) gives:

$$i_{dr\,ps} = -(2cp_{\perp 0}/B_{ps0}) - 2c\int_d^D (1/B_{ps})(\partial p_{\perp}/\partial z)\,\mathrm{d}z \tag{12}$$

where $p_{\perp 0}$ and $B_{ps0}$ are the pressure and field intensity just above the neutral sheet, $d$ and $D$ are half-thicknesses of the neutral and plasma sheets respectively. The sum of currents (10) and (12) is the net drift current per unit length of the neutral-sheet/plasma-sheet system:

$$i_{dr} = i_{dr\,ns} + i_{dr\,ps} = (2c/B_{ps0})(p_{\parallel 0} - p_{\perp 0}) - 2c\int_d^D (1/B_{ps})(\partial p_{\perp}/\partial z)\,\mathrm{d}z. \tag{13}$$

Since we neglect the gradients $\partial/\partial x$ with respect to $\partial/\partial z$, the net magnetization is evident from (8) to be zero (the integration paths $ab$ and $cd$ lie now outside the plasma sheet); thus (13) is the total current per unit tail length. The first term on the right approximately equals the net current in the neutral sheet given by (4) and the last term is an additional current in the rest of the system; since the pressure $p_{\perp}$ decreases towards the boundaries, this quantity is also positive.

## 4. A POSSIBLE SOURCE OF THE PLASMA-SHEET ANISOTROPY

The purpose of this section is to obtain a pitch-angle distribution of particles leaking from the isotropic neutral sheet in a simple field model. We shall study in detail the motion of protons crossing the boundaries between the neutral and plasma sheets. These boundaries are defined as a pair of conventional planes (Fig. 4), confining a region of weak magnetic field which has here a vertical component $B_z$ only. The particles move inside the neutral sheet in a random way, being thus distributed isotropically in velocity space. The field outside this region has also a horizontal component $B_x$ which is several times greater than $B_z$, and corresponds to a thick plasma-sheet field depression.

Consider a proton with velocity $\vec{v}$ crossing the plane at point A, from inside the neutral sheet. Let us denote by $\varphi$ the angle between the line BB′ (lying in the $xz$-plane and normal to the field line AC), and the velocity component $\vec{v}_{\perp}$, normal to AC. There exist two possibilities, depending on values of $\varphi$ and the pitch-angle $\theta$. In the first case the particle

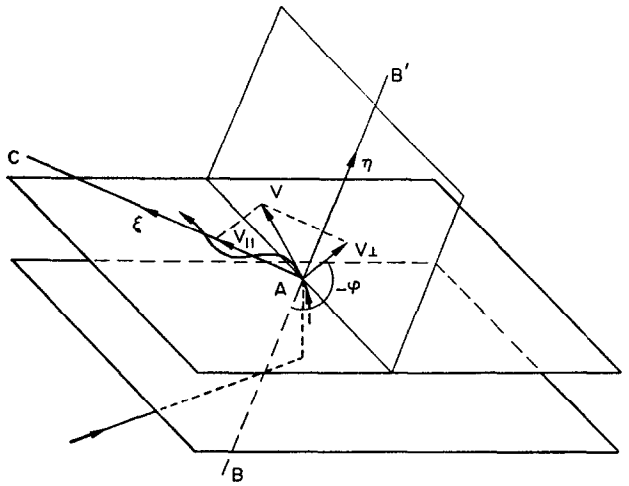


FIG. 4. THE NEUTRAL SHEET MODEL (FOR THE DERIVATION OF THE PITCH-ANGLE DISTRIBUTION FUNCTION IN THE PLASMA SHEET).

immediately crosses the plane again and returns into the neutral sheet; the second possibility (realized, for example, in the case of small pitch-angles) is to move along the field line. Since the particles of the second type form the plasma sheet, we can calculate its distribution function, assuming the latter, for any given $\theta$, to be proportional to the interval of $\varphi$ which corresponds to the second possibility. If $\varphi = 0$, the ejection condition is simply:

$$\tan\theta = v_\perp/v_\parallel < B_z/B_x. \tag{14}$$

Other values of $\varphi$ require a little more calculation. For example, let us consider the case $\varphi = \pi$. Introducing a coordinate system centered at point A, with its $\xi$-axis along the field line AC and $\eta$-axis along AB′ (Fig. 4), we obtain the equation of the ejected particle trajectory, projected on the $\xi\eta$-plane:

$$\eta = R_L \sin(\omega_L \xi/v_\parallel)$$

where $\omega_L = (eB_{ps}/mc)$ and $R_L = v_\perp/\omega_L$ are the gyrofrequency and gyroradius in the plasma sheet, respectively. It is easy to find that the lowest point of this curve (in the $xyz$-system) is achieved, when:

$$(\omega_L \xi/v_\parallel) = \pi + \arccos(B_z v_\parallel/B_x v_\perp).$$

The particle will be ejected, if this point is above the neutral-sheet boundary, i.e. $|\eta| < (B_z/B_x)\xi$, which condition yields:

$$[1 - (B_z v_\parallel/B_x v_\perp)^2]^{1/2} < (B_z v_\parallel/B_x v_\perp)[\pi + \arccos(B_z v_\parallel/B_x v_\perp)]. \tag{15}$$

Denoting $B_z v_\parallel/B_x v_\perp = \cos\beta$, we rewrite (15) as:

$$\tan\beta < \pi + \beta.$$

The last inequality is satisfied if $\beta < 77{\cdot}5°$, so that

$$\tan\theta < 4{\cdot}63(B_z/B_x). \tag{16}$$

Carrying out the calculations for other values of $\varphi$ between 0 and $\pi$ in a similar manner, we generalize the ejection condition of type (14) and (16) in the following way:

$$\tan\theta < f(\varphi)(B_z/B_x). \tag{17}$$

It can also be shown (see Appendix), that

$$f((\varphi) \approx \frac{(\pi/2) + \varphi}{1 + \sin \varphi}, \qquad \text{if } \pi \leq \varphi < (\tfrac{3}{2})\pi \tag{18}$$

with accuracy better than 2 per cent, and:

$$f(\varphi) = (\cos \varphi)^{-1} \quad \text{if} \quad (\tfrac{3}{2})\pi < \varphi \leqslant 2\pi. \tag{19}$$

Thus $f(\varphi)$ has a singularity when $\varphi = (\frac{3}{2})\pi$. This means that all pitch-angles are 'permitted' near this value of $\varphi$.

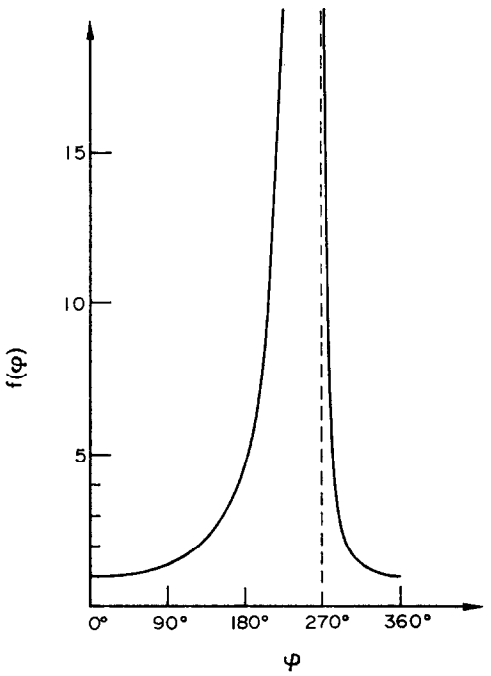


FIG. 5. PLOT OF THE FUNCTION $f(\varphi)$ FROM THE EJECTION CONDITION (17).

Now, having a plot of $f(\varphi)$, shown in Fig. 5, we can find graphically, for any $\theta$, an interval $\Delta\varphi$ inside which (17) is satisfied, and so obtain the distribution function $F(\theta)$ in the plasma sheet. Figure 6 shows the functions $F(\theta)$ derived for three values of the relative magnitude of the vertical field component, curves 1, 2 and 3 corresponding to $B_x/B_z = 20$, 10 and 5 respectively. The dashed line above corresponds to an isotropic plasma sheet (so, in fact, $F(\theta)$ is a differential flux rather than the usual pitch-angle distribution function; to get the latter, one should multiply $F(\theta)$ by $\sin \theta$).

We see that field-aligned particle fluxes of angular width $\sim 2 \arctan (B_z/B_x)$ are formed in our model. The mechanism described is essentially non-adiabatic, so one may expect it to be effective with respect to protons only, though a more rigorous treatment should incorporate the coupling of particles of both species.

It is of interest to calculate the ratios $p_\parallel/p_\perp$ for the distributions of Fig. 6. A numerical integration was performed to obtain the values of

$$p_\parallel/p_\perp = 2\int_0^{\pi/2} \sin \theta \cos^2\theta F(\theta)\, d\theta \Big/ \int_0^{\pi/2} \sin^3\theta F(\theta)\, d\theta. \tag{20}$$

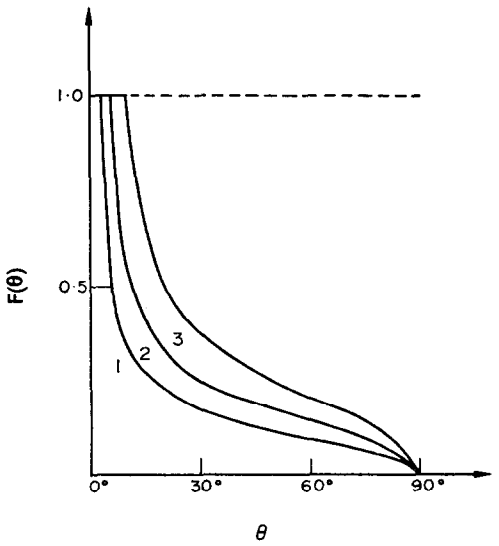


FIG. 6. PITCH-ANGLE DISTRIBUTIONS OF THE EJECTED PROTONS FOR THREE VALUES OF THE RATIO $B_x/B_z = 20$, 10 AND 5 (CURVES 1, 2 AND 3, RESPECTIVELY).

In the same three cases ($B_x/B_z = 5$, 10 and 20), we have found $p_\parallel/p_\perp = 2{\cdot}30$, $2{\cdot}15$ and $2{\cdot}11$ respectively. Note that these values are of the same order as the estimate $p_\parallel/p_\perp \approx 1{\cdot}6$ of Section 3, and are practically independent of the relative magnitude of the normal field component in the neutral sheet.

## 5. DISCUSSION AND CONCLUSIONS

We have treated above a static model plasma sheet without any electric fields, in contrast with the reconnection theory. Experimental data show this assumption to be reasonable, at least for quiet conditions, when there exists neither direct, nor indirect evidence of the large-scale electric field in the magnetotail.

Starting from the steady-state assumption, we came to the conclusion that a substantial anisotropy ($p_\parallel/p_\perp \approx 1{\cdot}6$) is necessary to maintain the tension balance in the plasma sheet. Besides that, one might suggest solar-wind momentum as a possible cause of the field-line stretching. However, in the near tail ($X_{SM} \gtrsim -40R_E$), it seems unlikely the stream will penetrate into the plasma sheet (Dessler, 1968). Recent experiments by Hones *et al.* (1972) confirm this point of view, since the average plasma-flow direction at the Vela orbit appears to be earthward.

It was shown that the neutral sheet itself can be a source of anisotropic proton fluxes in the plasma sheet. The pitch-angle distribution derived in the simple model has the ratio $p_\parallel/p_\perp \sim 2{\cdot}2$, almost independent of the relative magnitude of the vertical field component. It is to be noted, however, that our speculations are rather schematic, and a more complete analysis is desirable, which would include the coupling of protons with electrons, and the possible effects of charge separation. In this connection a work by Cowley (1971) should be mentioned which is restricted, however, to the case of $B_z = 0$.

Other possible sources of the anisotropy should be kept in mind, of course. Speiser (1965, 1967) has shown that the neutral-sheet particles accelerated by the cross-tail electric field could form field-aligned beams with small pitch angles. This mechanism may be most

effective near the inner edge of the plasma sheet, where the electric field should be sufficiently intense, especially during magnetospheric disturbances. Hones *et al.* (1971) proposed that ionospheric particles could be responsible for the observed field-aligned beams. One more possible reason for the plasma-sheet anisotropy can be pointed out, specifically the drift-shell splitting due to the noon–midnight asymmetry of the geomagnetic field (Roederer, 1967). Dayside particles with pitch angles within the drift loss cone will come to the stretched magnetotail field lines during their motion around the Earth. Assuming the particle magnetic moment to be preserved, we have for its pitch angle $\theta_{ps}$ in the plasma sheet:

$$\sin \theta_{ps} = \sin \theta_{ds}(B_{ps}/B_{ds})^{1/2} \tag{21}$$

where the subscripts *ps* and *ds* refer to the plasma sheet and the dayside magnetosphere, respectively. Since, by order of magnitude, $B_{ps} \sim 0{\cdot}1 B_{ds}$, we obtain roughly:

$$\sin \theta_{ps} \sim (\tfrac{1}{3}) \sin \theta_{ds}$$

i.e. a 'stretch' of the distribution function along the field lines (Mead, 1966). The influx of anisotropic plasma into the sheet may be increased greatly during the stormtime compression of the dayside magnetosphere, due to an enhancement of pitch-angle scattering into the drift loss cone, and a more effective penetration of the solar-wind plasma through the dayside cusps. The corresponding increase in $p_{\|}$ can lead to an intensification of the tail current system in accordance with (4) and, hence, to an increase in the tail-field magnitude and its magnetic flux, observed experimentally. On the other hand, the enhanced anisotropy can give rise to an instability in the plasma sheet.

## REFERENCES


ALEXEEV, I. I. and KROPOTKIN, A. P. (1970). Interaction of energetic particles with the neutral layer of the magnetosphere tail. *Geomagn. Aeron.* **10,** 777.

BEARD, D. B., BIRD, M. and JAO, HUI HUANG (1970). Self-consistent theory of the magnetotail. *Planet. Space Sci.* **18,** 1349.

BEHANNON, K. W. (1970). Geometry of the geomagnetic tail. *J. geophys. Res.* **75,** 743.

COWLEY, S. W. H. (1971). The adiabatic flow model of a neutral sheet. *Cosmic Electrodynamics* **2,** 90.

DESSLER, A. J. (1968). Magnetic merging in the magnetospheric tail. *J. geophys. Res.* **73,** 209.

FAIRFIELD, D. H. and NESS, N. F. (1970). Configuration of the geomagnetic tail during substorms. *J. geophys. Res.* **75,** 7032.

HILL, T. W. and DESSLER, A. J. (1971). Plasma-sheet structure and the onset of magnetospheric substorms. *Planet. Space Sci.* **19,** 1275.

HONES, E. W., JR., ASBRIDGE, J. R., BAME, S. J. and SINGER, S. (1971). Energy spectra and angular distributions of particles in the plasma sheet and their comparison with rocket measurements over the auroral zone. *J. geophys. Res.* **76,** 63.

HONES, E. W., JR., ASBRIDGE, J. R., BAME, S. J., MONTGOMERY, M. D., SINGER, S. and AKASOFU, S.-I. (1972). Measurements of magnetotail plasma flow made with Vela 4b. *J. geophys. Res.* **77,** 5503.

LONGMIRE, C. L. (1963). *Elementary Plasma Physics.* Interscience, New York.

MEAD, G. D. (1966). The motion of trapped particles in a distorted field. *Radiation Trapped in the Earth's Magnetic Field,* p. 481. Reidel, Dordrecht, Holland.

NESS, N. F., SCEARCE, C. S. and SEEK, J. B. (1964). Initial results of the IMP 1 magnetic field experiment. *J. geophys. Res.* **69,** 3531.

RICH, F. J., VASYLIUNAS, V. M. and WOLF, R. A. (1972). On the balance of stresses in the plasma sheet. *J. geophys. Res.* **77,** 4670.

ROEDERER, J. G. (1967). On the adiabatic motion of energetic particles in a model magnetosphere. *J. geophys. Res.* **72,** 981.

SCHINDLER, K. (1972). A self-consistent theory of the tail of the magnetosphere. *Earth's Magnetospheric Processes* (Ed. B. M. McCormac). Reidel, Dordrecht, Holland.

SHABANSKY, V. P. (1971). Some processes in the magnetosphere. *Space Sci. Rev.* **12,** 299.

SISCOE, G. L. (1972). Consequences of an isotropic static plasma sheet in models of the geomagnetic tail. *Planet. Space Sci.* **20,** 937.

SPEISER, T. W. (1965). Particle trajectories in model current sheets—I. Analytical solutions. *J. geophys. Res.* **70**, 4219.
SPEISER, T. W. (1967). Particle trajectories in model current sheets—II. Applications to auroras using a geomagnetic tail model. *J. geophys. Res.* **72**, 3919.

## APPENDIX

The equation of a particle trajectory, projected on the $\xi\eta$-plane, in the case of arbitrary $\varphi$, can be written as follows:

$$\eta = -R_L \sin\varphi + R_L \sin(\omega_L \xi/v_\parallel + \pi - \varphi). \tag{A1}$$

In the interval $\pi \leqslant \varphi < (\frac{3}{2})\pi$ it can be assumed that the trajectory point, nearest to the neutral sheet boundary approximately corresponds to the first minimum value of $\eta$, i.e.

$$\omega_L \xi/v_\parallel + \pi - \varphi \approx (\tfrac{3}{2})\pi. \tag{A2}$$

The maximum error of such approximation is achieved by $\varphi = \pi$, where the exact value of the function $f(\varphi)$ was shown above to be equal to 4·63. The ejection condition $|\eta| < (B_z/B_x)\xi$, combined with (A1) and (A2) lead to:

$$R_L(1 + \sin\varphi) \leqslant (B_z/B_x)(v_\parallel/\omega_L)(\pi/2 + \varphi) \tag{A3}$$

from which relation (18) immediately follows. The maximum error is equal to $(\frac{3}{2})\pi - 4{\cdot}63 \approx 0{\cdot}08$, i.e. less than 2 per cent.

In the interval $(\frac{3}{2})\pi < \varphi \leqslant 2\pi$ the only restriction on pitch angles is that the velocity component, normal to the neutral sheet boundary, must be positive, i.e. directed upward in Fig. 4. Thus

$$v_z = v_\parallel(B_z/B_{ps}) - v_\perp \cos\varphi\,(B_x/B_{ps}) > 0 \tag{A4}$$

and, hence

$$\tan\theta < (1/\cos\varphi)(B_z/B_x)$$

in accordance with (19).